JOURNAL OF SOLID STATE CHEMISTRY 19, 227–233 (1976)

The Stability of the Perovskite-Type Zirconium Tungsten Bronze Zr_xWO_3.

THOMMY EKSTRÖM

Department of Inorganic Chemistry, Arrhenius Laboratory, University of Stockholm, S 104 05 Stockholm, Sweden

AND R. J. D. TILLEY

School of Materials Science, University of Bradford, Bradford BD7 1DP, West Yorkshire, England

Received May 3, 1976; in revised form June 21, 1976

It has been found that a perovskite-related zirconium tungsten bronze Zr_xWO_3 (with $0 < x \leqslant 0.08$) forms readily at temperatures between 973 and 1573° K. Prolonged heating causes the bronze to decompose to other oxide products at all the temperatures investigated. These results are summarized in phase diagrams. Possible reasons for the decomposition of the bronze are discussed.

Introduction

Chang, Scroger, and Phillips (*1*) were the first to report the existence of another ternary oxide besides ZrW_2O_8 in the ZrO_2–WO_2–WO_3 system at temperatures above 1573°K. The composition of the new oxide seemed to vary somewhat and an extended phase range with $x \approx 0.05$–0.09 in either of the two formulas $Zr_xW_{1-x}O_{2.9-0.9x}$ or $Zr_xW_{1-x}O_{3(1-x)}$ was suggested. The first of these formulas describes a range of homogeneity along the ZrO_2–$W_{20}O_{58}$ line in the phase diagram and the latter along the Zr–WO_3 line. The X-ray powder pattern of the new oxide was readily indexed in the terms of a cubic unit cell that resembled that of ReO_3, and the authors suggested that the ternary phase found might be related to the well-known A_xWO_3 tungsten bronzes formed by the alkali group metals.

Later studies by the present authors (*2*) at lower temperatures 1273–1373°K confirmed the findings by Chang *et al.* and showed that the extended homogeneity range of the new oxide was only along the Zr–WO_3 line in the phase diagram. This oxide was, therefore, a perovskite-related bronze Zr_xWO_3. For low x values the symmetry of the Zr_xWO_3 bronze was found to be monoclinic, but passed through orthorhombic to tetragonal (pseudocubic) as the zirconium content increased. The pseudocubic bronze was found within the composition interval $x \approx 0.047$–0.075 and the X-ray powder pattern was very like that of cubic ReO_3 with a small shift in the line positions caused by a slightly changed unit cell parameter. It was, however, possible with the high-resolution Guinier–Hägg cameras to see a splitting of the pseudocubic bronze high-angle reflections that revealed a tetragonal unit cell.

As the results obtained by the X-ray and electron diffraction techniques presented in our previous communication did not reveal any evidence for the position of the Zr atoms in the WO_3 host structure that might account for the formation of the Zr_xWO_3 bronze, additional studies of the bronze were initiated. The results of these extended investigations are presented below.

Experimental

Details of the starting materials, the preparation techniques, and the X-ray and electron microscopy analysis have been given in an earlier publication (*2*). In this study the samples heated at high temperatures or for long heating times were, however, sealed

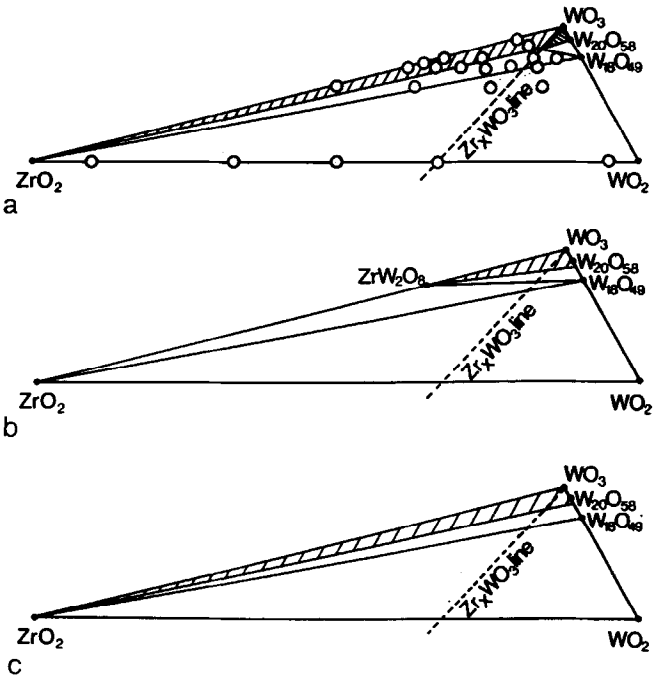

FIG. 1. (a) Nonequilibrium phase relations in the dioxide–trioxide region of the Zr–W–O system for samples heated for relatively short times in the temperature interval 973–1573° K. The open circles represent gross compositions of samples prepared in this study, except for samples on the Zr_xWO_3 line ($0 < x < 0.10$) which have been omitted for clarity. (b) Equilibrium phase-relationships at temperatures above about 1380° K, where the ZrW_2O_8 oxide is stable. (c) Equilibrium phase-relationships at temperatures below about 1380° K, where the ZrW_2O_8 oxide is unstable. The hatched areas represent regions where equilibrium is between two phases in which one is of continuously variable composition.

within evacuated Pt tubes. For the lowest temperature employed in this study, 973°K, the heating times were up to 4 months in duration. At the highest temperature used, 1573°K, the longest heat-treatment used was 2 weeks. At intermediate temperatures, 1073, 1273, and 1373°K, heating times between these extremes were chosen. The samples prepared were mainly of gross composition Zr_xWO_3 ($0.01 \leqslant x \leqslant 0.10$), but other samples in the composition region ZrO_2–WO_2–WO_3 were also utilized to clarify some aspects of the results. The composition of these samples are shown in Fig. 1a.

Results

X-Ray Analysis

At all temperatures studied the bronze was found to form relatively rapidly. In addition to the structures reported earlier (*2*), both the high-temperature preparations and the lower-temperature preparations heated for long times, yielded a cubic form of the Zr_xWO_3 bronze. This cubic phase seems to have a very narrow composition range at about $x = 0.08$, which is the highest Zr content observed in this series of bronzes. The cell size of the cubic bronze did not vary and the X-ray powder pattern was readily indexed with the parameter $a = 3.775$ (± 1) Å. A very small single crystal of the cubic bronze was investigated using the Weissenberg X-ray technique and the results thus obtained confirmed the symmetry and the cell size. It was also observed that the room temperature X-ray powder patterns of the bronze phase occurring in samples of one particular composition, but heated at different temperatures, showed no significant differences. The general appearance of the phase

TABLE I

A COMPARISON OF SOME PHASE ANALYTICAL DATA FOR THE Zr_xWO_3 SYSTEM OBTAINED FROM X-RAY POWDER PATTERNS OF SAMPLES HEATED FOR DIFFERENT TIMES AT ELEVATED TEMPERATURES

Gross composition Zr_xWO_3, where $x =$	Heated at 1373° K		Heated at 1573° K		Heated at 973° K
	1 week	6 weeks	12 hours	1 week	4 months
0.02	*M*[a]	*M*, *O*, WO_{3-y}	*M*, *O*, WO_{3-y}	WO_{3-y}, (ZrW_2O_8)	*M*, (WO_{3-y})
0.04	*O*	*O*, *M*	*O*, *M*, (*T*)	WO_{3-y}, (ZrW_2O_8)	*O*, (*M*), ((*E*))
0.06	*T*	*T*, *O*, (*E*)	*T*, (*O*),	WO_{3-y}, (ZrW_2O_8)	*T*, *O*, (*E*)
0.08	*T*, (($W_{18}O_{49}$))	*C*, (*E*), ((ZrO_2))	*C*	WO_{3-y}, ZrW_2O_8	*C*, ((*E*))
0.10	*T*, ($W_{18}O_{49}$), ((ZrO_2))	*C*, (*E*), (ZrO_2)	*C*, (ZrW_2O_8)	WO_{3-y}, ZrW_2O_8, ($W_{18}O_{49}$)	*C*, (*E*), ((ZrO_2))

[a] The following capital letters are used to denote the different symmetries of the observed Zr_xWO_3 bronze: *M* = monoclinic, *O* = orthohombic, *T* = tetragonal (pseudocubic), and *C* = cubic. The capital letter *E* is used to denote a new oxide thought to have a composition close to ZrW_2O_8. The parentheses, ( ) and (( )), mean small amounts and very small amounts of a phase, deduced from X-ray line intensities.

diagram thus obtained for the samples heated for short times is summarized in Fig. 1a.

After long heating times the Zr_xWO_3 bronze was found to decompose at all the temperatures investigated. The bronze is therefore metastable, but the rate of decomposition is very slow at lower temperatures. This is exemplified by the fact that samples heated for 2 weeks at 1373° K give no clear evidence for initial decomposition and times of about 3–4 weeks are needed before the decomposition is observed by X-ray powder diffraction. However, the bronze heated at the highest temperature, 1573°K, showed X-ray evidence for a decomposition at low x-values after only 12 hr heating. A set of phase analytical data obtained after long heat-treatment at different temperatures are compared with the results obtained by shorter heating times in Table I.

A general trend observed for all temperatures is that the Zr_xWO_3 bronze with the lowest x-values decomposes initially into two phases. There is a clear segregation of the Zr to form a Zr-richer bronze and a Zr-poorer bronze. The bronze of greatest stability seems thus to be the cubic form at $x \approx 0.08$, although complete segregation to only the cubic form is only rarely achieved. After heating for about 1 week at 1573°K the Zr-rich bronzes also decompose into the oxide ZrW_2O_8 and binary tungsten oxides WO_{3-y}. In Fig. 1b the phase diagram thus obtained at this temperature is illustrated.

As the ZrW_2O_8 oxide is not formed or else is not stable at temperatures below about 1380°K (*1*, *3*), the Zr_xWO_3 bronze heated at 1373°K and lower temperatures did not decompose to yield the ZrW_2O_8 oxide as the Zr-bearing phase. Instead the X-ray powder pattern of another Zr-rich oxide, *E*, was observed (see Table I). This oxide was always present in fairly low concentrations when the Zr-rich bronze had decomposed and it seemed to contain all the Zr released by the decomposition. This oxide, however, apparently formed in a metastable state as it seemed to gradually decompose upon prolonged heating into ZrO_2 and tungsten oxides. The final equilibrium at temperatures below 1380°K was hence found to be between ZrO_2 and appropriate binary tungsten oxides which contain variable numbers of more or less well-ordered *CS* planes (cf. Fig. 1c). Thus, the initial stage of bronze decomposition at low temperatures is rather similar to that at high temperatures. The difference lies mainly in the relative stabilities of ZrW_2O_8 and the *E* phase.

Additional phase analytical work at gross compositions other than on the Zr_xWO_3 line

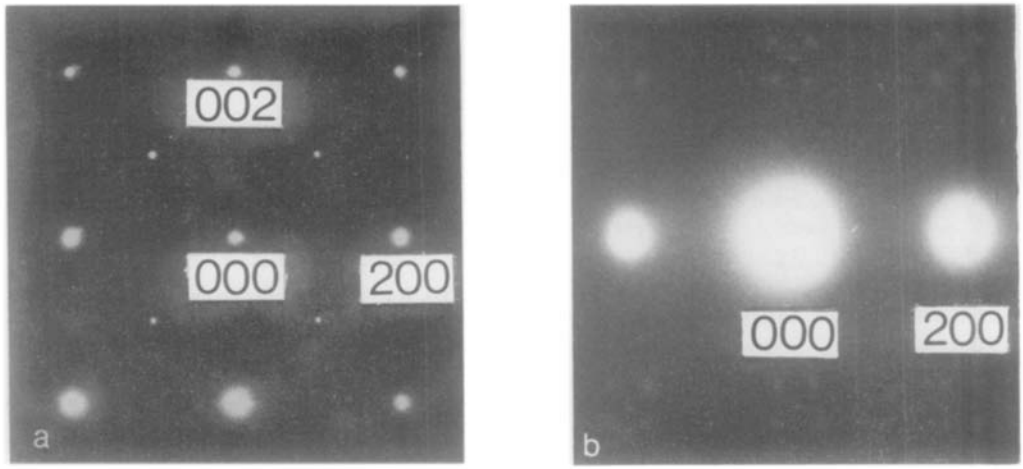

FIG. 2. Electron diffraction patterns from a crystal of a Zr_xWO_3 pseudocubic bronze. (a) *h0l* reciprocal lattice section, (b) the *h0l* section tilted by approximately 11° about the *h*00 row, showing diffuse scattering above and below the *h0l* plane.

showed that the oxide *E* was also found in small amounts in preparations made in the pseudobinary ZrO_2–WO_3 system, although the true equilibrium at the temperature 1373°K and below clearly lies between the two end-members ZrO_2 and WO_3. The preparations also revealed that the oxide *E* formed preferentially in samples of gross compositions around ZrW_2O_8. From these data it seems possible that *E* is a metastable oxide of a composition close to that of ZrW_2O_8 which forms at temperatures below the decomposition temperature of the high-temperature phase. The X-ray powder data obtained from X-ray films containing other phases are given in Table II. One way to index the pattern is to select a tetragonal cell with dimensions $a = 14.012\ (\pm 2)$ Å and $c = 5.726\ (\pm 2)$ Å. However, this must be regarded as only a preliminary possibility until single-crystal data become available and for this reason the data given in Table II have not been indexed.

Electron Microscopy

The electron microscope study confirmed our earlier finding that no *CS* formation takes place in the Zr_xWO_3 bronze phase range (*2*). In addition, an examination of the samples heated for longer times and at higher temperatures showed that slightly reduced $WO_{3-\delta}$ crystals containing disordered {102} *CS* planes were present in specimens in which the bronze had begun to decompose. Some crystal fragments of the bronze with tetragonal symmetry

TABLE II

THE X-RAY POWDER PATTERN OF A METASTABLE PHASE THOUGHT TO HAVE A COMPOSITION CLOSE TO ZrW_2O_8, WHICH FORMS PREFERENTIALLY BY THE DECOMPOSITION OF THE Zr_xWO_3 BRONZE AT 1373°K AND LOWER TEMPERATURES

Intensity	*d* (Å)
m	4.432
s	3.300
vvw	2.747
vw	2.650
s	2.518
m	2.337
w	2.216
s	2.067
m	1.908
m	1.752
s	1.712
m	1.652
w	1.495
m	1.477
s	1.381

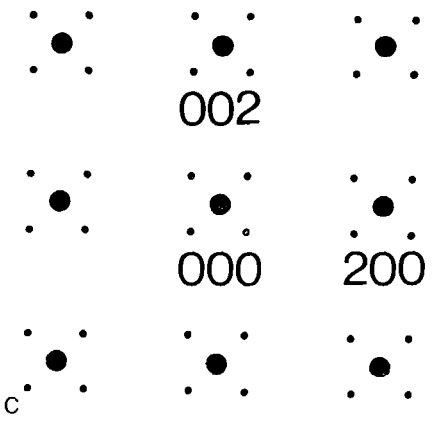

Fig. 2. (c) Diagram showing the positions of extra reflections expected if {111} twins were present in a cubic crystal. The large spots are the matrix reflections and the small spots, which lie above and below the *h*0*l* plane on the cube body diagonals, are due to the presence of the twins.

were also twinned on the pseudocubic {111} planes, which suggests that at the preparation temperature the symmetry may be cubic, and that twinning takes place as the samples cool. Further high-temperature studies are needed to check this however, as other explanations are also possible (*vide infra*).

As reported earlier, the majority of the crystal flakes examined showed a confused diffraction contrast which was interpreted as being due to microdomains of differing Zr concentration in the bronze crystals. Such crystals also showed a distinctive pattern of diffuse scattering around the main WO_3 reflections. This diffuse scattering does not lie in the {*hk*0} planes but above and below them at the corners of a small cube centred upon the main {*hk*0} reflections, so that it is only recorded upon diffraction patterns when the crystal is tilted about one of the directions [100], [010] or [001], as shown in Figs. 2a and 2b. Initially it was believed that the diffuse scattering arose from short-range ordering of the Zr atoms, but the presence of the same features in crystals heated for several months, and the absence of any strongly developed superlattice reflections related to the diffuse scattering makes it necessary to reappraise this conclusion. A further analysis of the geometry of these diffuse reflections has therefore been made, and within the normal accuracy of electron microscope goniometer stages it was found that the diffuse reflections lie near positions expected for extra reflections due to double-diffraction from {111} twins in a cubic or pseudocubic crystal (*4*). This suggests that a more likely model to account for the presence of the diffuse scattering is to consider that the crystal matrix contains very small twinned regions lying upon {111} planes. In such a case the twin spots, which normally lie on the body diagonals of the reciprocal lattice, would be extended in reciprocal space, allowing them to be detected at positions closer to the {*hk*0} plane than usually expected. This model is in good agreement with the geometry of the diffraction patterns, as can be seen by comparing Fig. 2c with Figs. 2a and 2b. In Fig. 2c the positions of the extra reflections due to {111} twins are projected onto the (*hk*0) plane of the reciprocal lattice. The positions of these spots are very close to the positions of the diffuse reflections in Fig. 2b. Such structural defects would contribute to the confused electron diffraction contrast observed, but a more detailed analysis of the diffraction effects is needed before a precise structural cause can be suggested. As this is not central to our purpose in this study it has not been made.

Discussion

The results described in this paper show that although a perovskite bronze Zr_xWO_3 forms rapidly in the Zr–W–O system for gross compositions near to WO_3 it is unstable and decomposes to other products. The overall scheme of the reaction seems to be a rapid diffusion of Zr atoms into the WO_3 host structure to give a crystal macroscopically uniform but containing coherently intergrown microdomains of differing Zr concentrations on a microscopic scale. These initial reaction products separate into two components, a Zr-rich bronze, of composition near to $Zr_{0.08}WO_3$ and a Zr-poor bronze of composition near to WO_3. Further Zr enrichment forms the phase ZrW_2O_8 at high temperatures and a phase of similar but as yet

unknown composition or structure at lower temperatures.

At present it is not possible to give quantitative reasons for the unstable nature of the Zr_xWO_3 bronze phase. Four factors are commonly cited in qualitative discussions of stability of such bronzes; the size, coordination number and geometry of the interpolated ions, and the electron structure of the bronze, although all of these factors are merely different aspects of the outer electron structure of the ions involved in the bronze reaction. The coordination number of Zr is 7 or 8 in its binary dioxide modifications (*5–7*). Indeed Zr^{4+} has a great preference for such unusual coordination numbers and a coordination geometry of a distorted trigonal prismatic type. We can assume that it is this which militates against an octahedral coordination and the consequent formation of *CS* phases as its near neighbor Ti prefers (*8*). Size is also of some importance in this matter, for the radius of the Zr^{4+} ion is somewhat larger than the Ti^{4+} ion (*9*) making the octahedral site less favorable for zirconium. As the outer electron structures of Ti and Zr atoms are the same, apart from a difference of 1 in the principal quantum number, other electron effects should not be of overriding importance.

Although the size of the ion and its chemical behavior in oxides suggests that Zr ions will not favor octahedral coordination, the same considerations lead one to expect that the Zr ions will be equally unsuited to the 12 coordination to be found in the only other reasonable site for the Zr atoms to occupy, the large cages between the WO_6 octahedra. The Zr^{4+} ion will be rather small in this case, and the possibility of lower valence Zr ions existing in the bronze has been ruled out by measurements of magnetic susceptibility which show only a very small temperature independent (Van Vleck) paramagnetism (*10*). Thus at the simplest level, the two most likely sites for Zr ion occupation in the perovskite bronze structure seem to be somewhat unfavorable for the Zr ions and we can suggest that this has an important bearing on the lack of stability of these compounds.

The electron microscope results suggest that the Zr atoms are partially able to overcome this problem of coordination geometry by an involvement with the twinned regions in the bronzes. As described earlier, the twinned regions in the typical Zr_xWO_3 bronzes are small and disordered, producing no well-aligned arrays of microtwins which are commonly produced on quenching a high-temperature–high-symmetry phase to room temperature. A consideration of the geometry of the WO_3 structure reveals that {111} twins will generate either face sharing octahedra, if the twin plane is an oxygen plane, or a trigonal prism, if the twin plane coincides with a metal atom plane. These are shown in Fig. 3. Of the two, the trigonal prism arrangement is most likely in view of the coordination geometry preferences of Zr^{4+} ions. Hence we might expect the Zr^{4+} ions to be located in these twin planes, in trigonal prismatic coordination. The small twinned regions can then be regarded as small regions of a Zr-rich phase $(Zr,W)O_3$ which are completely coherently intergrown at random in the WO_3 structure.

This twinning is then a direct consequence of the Zr^{4+} ions, which are forcing the WO_3 lattice to accommodate it in a favorable

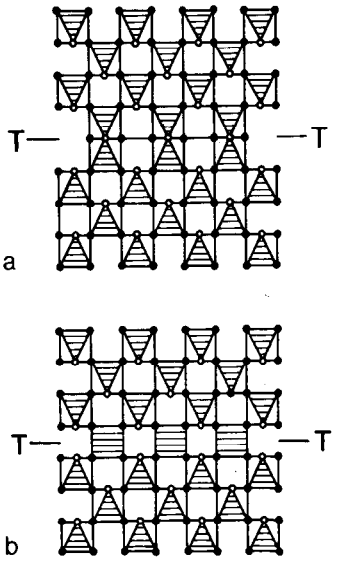

FIG. 3. {111} twin planes in the WO_3 structure consisting of (a) face sharing octahedra if the twin plane is an oxygen atom plane, or (b) trigonal prismatic coordination polyhedra if the twin plane coincides with a metal atom plane.

coordination position. Such twinning is likely to be energetically unfavorable. Twinning in WO_3 crystals has not been observed upon {111} planes in the past, only on {110} and {100} planes (*11*, *12*). Thus, as the Zr concentration in any particular crystal builds up, the unfavorable energy terms will increase, even if only a part of the Zr^{4+} ions are in twinned regions of the crystal. Ultimately this may provide the necessary driving force for the decomposition of the bronze and the nucleation of more stable Zr containing structures.

This suggestion needs further experimental evidence before it can be verified in detail. Such evidence may be obtained by a careful analysis of the electron optical image contrast or by diffraction studies designed to reveal whether the Zr^{4+} ions are clustered in any particular form. Until such additional evidence is available, the true microstructure of the Zr_xWO_3 bronzes must be open to some doubt and the reason for the instability of the bronze phase open to discussion.

Acknowledgments

R. J. D. T. is indebted to the Science Research Council (London) for an equipment grant. The research was also performed within a program supported by the Swedish Natural Science Research Council (T. E.). The authors would also like to thank Professor B. G. Hyde for an interesting discussion of structural relationships between ZrO_2 and WO_3.

References

1. L. L. Y. Chang, M. G. Scroger, and B. Phillips, *J. Amer. Ceram. Soc.* **50**, 211 (1967).
2. T. Ekström and R. J. D. Tilley, *Mater. Res. Bull.* **9**, 999 (1974).
3. J. Graham, A. D. Wadsley, J. H. Weymouth, and L. S. Williams, *J. Amer. Ceram. Soc.* **42**, 570 (1959).
4. P. B. Hirsch, A. Howie, R. B. Nicholson, D. W. Pashley, and M. J. Whelan, "Electron Microscopy of Thin Crystals," Chap. 6, Butterworths, London (1965).
5. J. D. McCullough and K. N. Trueblood, *Acta Crystallogr.* **12**, 507 (1959).
6. G. Teufer, *Acta Crystallogr.* **15**, 1187 (1962).
7. D. K. Smith and H. W. Newkirk, *Acta Crystallogr.* **18**, 983 (1965).
8. T. Ekström and R. J. D. Tilley, *Mater. Res. Bull.* **9**, 705 (1974).
9. R. D. Shannon and C. T. Prewitt, *Acta Crystallogr.* **B25**, 925 (1969).
10. B. Blom, Private communication.
11. S. Tanisaki, *J. Phys. Soc. Japan* **11**, 620 (1956); **13**, 363 (1958).
12. J. M. Berak and M. J. Sienko, *J. Solid State Chem.* **2**, 109 (1970).